HAL
open science

Quantum oscillations of a linear chain of coupled orbits with small effective masses: the organic metal θ-(BETS) 4 CoBr 4 (C 6 H 4 Cl 2)

Alain Audouard, Jean-Yves N Fortin, David Vignolles, Rustem I Lyubovskii, Loïc Drigo, Elena I Zhilyaeva, Rimma N Lyubovskaya

To cite this version:

Alain Audouard, Jean-Yves N Fortin, David Vignolles, Rustem I Lyubovskii, Loïc Drigo, et al.. Quantum oscillations of a linear chain of coupled orbits with small effective masses: the organic metal θ-(BETS) 4 CoBr 4 (C 6 H 4 Cl 2). 2017. hal-01462971

HAL Id: hal-01462971

https://hal.science/hal-01462971v1

Preprint submitted on 9 Feb 2017

HAL is a multi-disciplinary open access archive for the deposit and dissemination of scientific research documents, whether they are published or not. The documents may come from teaching and research institutions in France or abroad, or from public or private research centers.

L'archive ouverte pluridisciplinaire **HAL**, est destinée au dépôt et à la diffusion de documents scientifiques de niveau recherche, publiés ou non, émanant des établissements d'enseignement et de recherche français ou étrangers, des laboratoires publics ou privés.

Quantum oscillations of a linear chain of coupled orbits with small effective masses: the organic metal θ-$(BETS)_4CoBr_4(C_6H_4Cl_2)$

Alain Audouard,[1] Jean-Yves Fortin,[2] David Vignolles,[3] Rustem B. Lyubovskii,[4] Loïc Drigo,[3] Elena I. Zhilyaeva,[4] and Rimma N. Lyubovskaya[4]

[1] *Laboratoire National des Champs Magnétiques Intenses (UPR 3228 CNRS, INSA, UGA, UPS) 143 avenue de Rangueil, F-31400 Toulouse, France.*

[2] *Institut Jean Lamour, Département de Physique de la Matière et des Matériaux, CNRS-UMR 7198, Vandoeuvre-les-Nancy, F-54506, France.*

[3] *Laboratoire National des Champs Magnétiques Intenses (UPR 3228 CNRS, INSA, UJF, UPS) 143 avenue de Rangueil, F-31400 Toulouse, France.*

[4] *Institute of Problems of Chemical Physics, Russian Academy of Sciences, 142432 Chernogolovka, MD, Russia*

(Dated: February 9, 2017)

Abstract

De Haas-van Alphen (dHvA) and Shubnikov-de Haas (SdH) oscillations of the organic metal θ-$(BETS)_4CoBr_4(C_6H_4Cl_2)$ are studied in magnetic fields of up to 55 T at liquid helium temperatures. In line with Fermi surfaces (FS) illustrating the linear chain of coupled orbits, the observed Fourier components are linear combinations of the frequencies linked to the two basic orbits α and β, which have small effective masses compared to other organic metals with the same FS topology. Analytical formulas based on a second order development of the free energy within the canonical ensemble, not only account for the field and temperature dependence of the dHvA amplitudes but also for their relative values. In addition, strongly non-Lifshitz-Kosevich behaviours are quantitatively interpreted. In contrast, Shubnikov-de Haas oscillations are not accounted for by this model.

short title: Quantum oscillations of θ-$(BETS)_4CoBr_4(C_6H_4Cl_2)$

I. INTRODUCTION

Many charge transfer salts based on either the bis-ethylenedithio-tetrathiafulvalene (ET) or the bis-ethylenedithio-tetraselenafulvalene (BETS) molecule are organic metals. In many cases, their Fermi surface (FS) is an illustration of the linear chain of orbits coupled by magnetic breakdown (MB) which is the model FS proposed by Pippard to calculate MB amplitudes[1] (see the insert of Fig. 1). The first and most famous experimental realization of this FS was provided by the organic superconductor κ-$(ET)_2Cu(SCN)_2$[2,3]. In high enough magnetic fields, such FS give rise to quantum oscillations with a spectrum composed of linear combinations of the frequencies F_α and F_β linked, respectively, to the closed orbit α and to the MB orbit β, the area of which is equal to that of the first Brillouin zone (FBZ) (for a review, see e.g. Ref. 4). The point is that, in addition to the frequencies predicted by the semiclassical model of coupled orbits network by Falicov and Stachowiak[5,6], 'forbidden frequencies', such as $F_{\beta-\alpha}$ are observed in de Haas-van Alphen (dHvA) oscillations spectra. At variance with magnetoresistance, which in addition to Shubnikov-de Haas (SdH) oscillations can evidence quantum interference (QI) linked to *e.g.* the $\beta-\alpha$ QI path, dHvA oscillations are only sensitive to the density of states. Therefore, the $\beta-\alpha$ component should not be observed in dHvA spectra. Besides, field dependent amplitudes of few components linked to harmonics such as 2α and MB orbits such as $\beta+\alpha$ are not in agreement with the Falicov-Stachowiak model.

In addition to κ-$(ET)_2Cu(SCN)_2$[7], these issues have been recently addressed for θ-$(ET)_4CoBr_4(C_6H_4Cl_2)$[8] and θ-$(ET)_4ZnBr_4(C_6H_4Cl_2)$[9]. In the following, these two latter compounds are referred to as ET_4-Co and ET_4-Zn, respectively. In short, the field and temperature dependence of the observed Fourier components are accounted for by a second order development of the free energy within the canonical ensemble, in contrast to the LK formula which only involves a first order development. As a result, Fourier amplitudes can be expressed by second order polynomials in damping factors as reported in the appendix. As an example, the amplitude of the $\beta-\alpha$ component, which do not involve any classical orbit, is accounted for by second order terms only.

Here, we consider the charge transfer salt θ-$(BETS)_4CoBr_4(C_6H_4Cl_2)$. SdH oscillations of this strongly two-dimensional organic metal have been studied in magnetic fields of up to 14 T[10]. Reported oscillatory spectra evidence frequency combinations in agreement with the

above mentioned framework. The main feature of this organic metal is the small effective masses linked to the α and β orbits ($m_\alpha = 1.1$, $m_\beta = 1.9$) which are by a factor of about three smaller than for κ-$(ET)_2Cu(SCN)_2$ ($m_\alpha = 3$, $m_\beta = 6$, see Ref. 7 and references therein) allowing to check the model at high magnetic field with a set of parameters (effective masses and, as reported hereafter, MB field) strongly different from those of the compounds considered in previous studies. As reported in the following, unusual features are observed and nevertheless accounted for by the model.

II. EXPERIMENTAL

Crystals were synthesized by the standard electrocrystallization technique as reported in Ref. 11. They were studied in pulsed magnetic fields of up to 55 T with a pulse decay duration of 0.32 s. dHvA oscillations were measured through magnetic torque measurements of a crystal with approximate dimensions $0.1 \times 0.1 \times 0.04$ mm^3, stuck on a microcantilever. Variations of the microcantilever piezoresistance were measured at liquid helium temperatures with a Wheatstone bridge with an *ac* excitation at a frequency of 63 kHz. Magnetic torque amplitudes A_η^τ relevant to a given Fourier component η are related to the dHvA amplitude A_η by $A_\eta^\tau = \tau_0 B A_\eta$ where B is the magnetic field and τ_0 is a prefactor depending on the crystal mass, cantilever stiffness and tilt angle θ between the field direction and the normal to the conducting plane. Shubnikov-de Haas (SdH) oscillations were measured through contactless tunnel diode oscillator (TDO)-based method[8,12] on another crystal with approximate dimensions $1 \times 1 \times 0.04$ mm^3. The angle between the normal to the conducting plane and the magnetic field direction was $\theta = 10°$ for both crystals.

III. RESULTS AND DISCUSSION

Field-dependent TDO and magnetic torque data at 1.9 K, along with corresponding Fourier analysis, are reported in Fig. 1. Fourier spectra are composed of linear combinations of the two frequencies F_α and F_β, as it is the case of ET_4-Co[8] and ET_4-Zn[9], the Fermi surface of which illustrate the linear chain of coupled orbits (see the insert of Fig. 1). Fourier analysis yield $F_\alpha(\theta = 0) = 0.860 \pm 0.004$ kT and $F_\beta(\theta = 0) = 4.408 \pm 0.004$ kT, in agreement with low field data of Ref. 10, leading to $F_\alpha/F_\beta = 0.195$. This value is similar to those of ET_4-Co

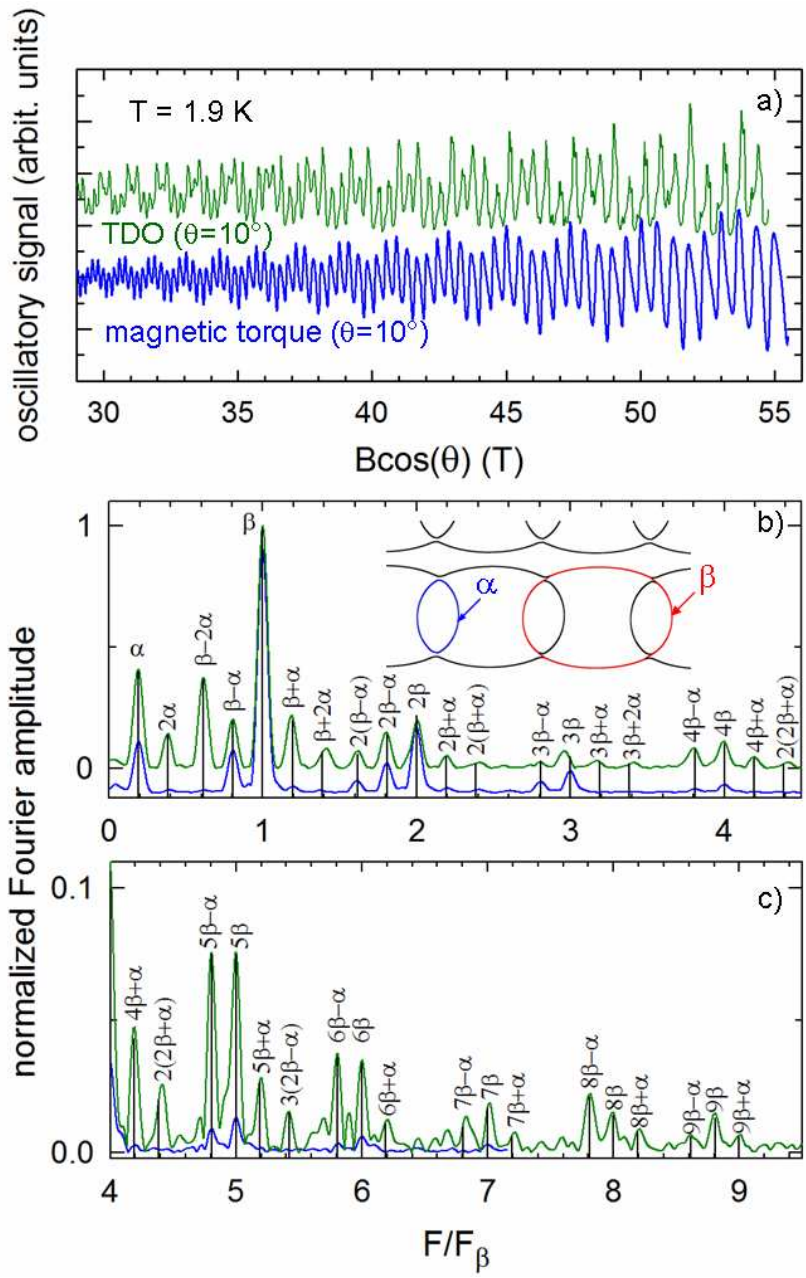

FIG. 1. (color on line) (a) Oscillatory part of the TDO and torque signal at 1.9 K and (b), (c) corresponding Fourier analysis for the field range 40-55 T (Fourier spectra are shifted down from each other for clarity). The angle between the field direction and the magnetic field is $\theta = 10°$. Thin lines in (b) and (c) are marks calculated with $F_\alpha(\theta = 0) = 0.86$ kT and $F_\alpha/F_\beta = 0.195$. The inset displays a sketch of the Fermi surface in which the basic orbits α and β are marked by blue and red lines, respectively.

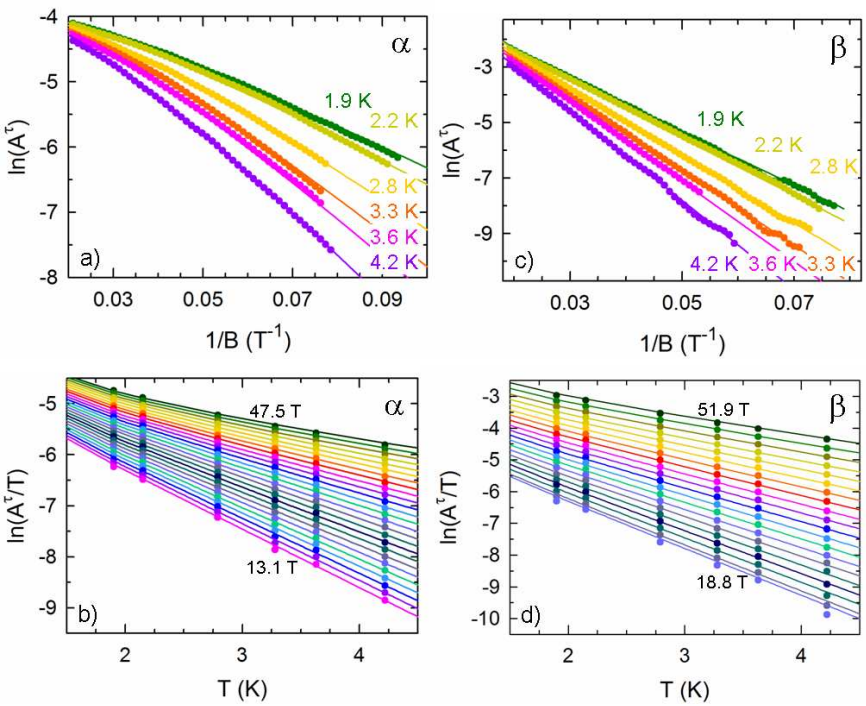

FIG. 2. (color on line) Dingle and mass plots of (a), (b) α and (c), (d) β components. Solid lines are best fits of Eqs. A.1 and A.2, respectively, to the data. They are obtained with $m_\alpha(\theta = 0) = 1.00$, $m_\beta(\theta = 0) = 1.88$, $B_0(\theta = 0) = 11.6$ T and $T_D = 0.66$ K. Uncertainty on these parameters is given in the text. Data of mass plots are obtained at magnetic field values evenly spaced in 1/B within the range indicated in (a) and (c).

and ET_4-Zn for which $F_\alpha/F_\beta = 0.206$ and 0.205, respectively. Compared to data relevant to these latter θ-phase compounds, an unprecedentedly large number of Fourier components can be observed, up to 6β ($F_{6\beta} = 26.4$ kT) and $9\beta + \alpha$ ($F_{9\beta+\alpha} = 40.6$ kT) for magnetic torque and TDO data, respectively.

Let us consider the magnetic torque data for which we will follow the process already adopted in Refs. 7–9. Recall that the amplitude (A_η) of the Fourier component with frequency $F_\eta = n_\alpha F_\alpha + n_\beta F_\beta$ is accounted for by analytic formulas given in the appendix. Briefly, provided the spin damping factors $R^s_{\alpha,1}$ and $R^s_{\beta,1}$ relevant to the basic components α and β are not close to zero, contributions of the second order terms of Eqs. A.1 and A.2 are negligible. As a result, these amplitudes are accounted for by the first order term, i.e. by the Lifshitz-Kosevich (LK) formula. In such a case, the spin damping factors act as temperature- and field-independent prefactors. Nevertheless, five independent parameters

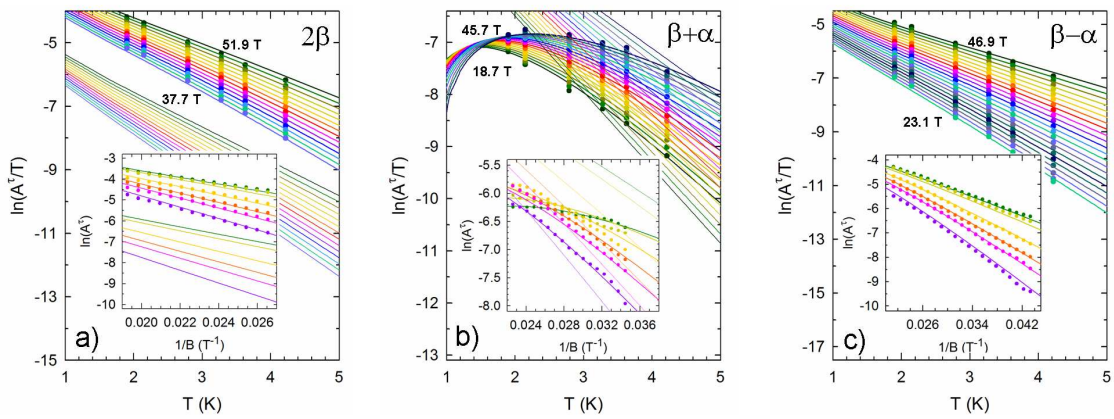

FIG. 3. (color on line) Mass plots of (a) 2β, (b) $\beta+\alpha$, and (c) $\beta-\alpha$ Fourier components. Data are evenly spaced in $1/B$ within the indicated field values. The inserts display the corresponding Dingle plots. Solid lines are best fits of Eqs. A.4, A.7 and A.5, respectively, to the data obtained with $m_\alpha(\theta=0)=1.00$, $m_\beta(\theta=0)=1.88$, $B_0(\theta=0)=11.6$ T and $T_D=0.66$ K (which are the same values as those deduced from the α and β components, see Fig. 2) and $g_\alpha=g_\beta=1.85$. Thin lines correspond to the contribution of the first order term (i.e. the Lifshitz-Kosevich formula).

still enter the amplitudes: the effective masses m_α and m_β, Dingle temperatures $T_{D\alpha}$ and $T_{D\beta}$ and the MB field B_0. For this reason, it is further assumed that the Dingle temperature is the same for both orbits ($T_{D\alpha}=T_{D\beta}=T_D$). These parameters having been determined from the data relevant to α and β, the effective Landé factors g_α and g_β can be determined from the data relevant to frequency combinations[7] or angle dependence of the amplitudes[9].

Field and temperature dependence of the α and β components amplitude is reported in Fig. 2. Best fits to the data yield $m_\alpha(\theta=0)=1.00\pm0.05$, $m_\beta(\theta=0)=1.88\pm0.08$ (in m_e units), $B_0(\theta=0)=11.6\pm3.2$ T and $T_D=0.66\pm0.10$ K. In agreement with the low field data of Ref. 10, effective mass values are very small compared to other organic metals with the same FS topology. MB field is significantly lower than for ET_4-Co ($B_0=35\pm5$ T) and ET_4-Zn ($B_0=26\pm3$ T), as well. Combination of small effective masses and MB field is certainly responsible for the very large number or frequency combinations observed in the data of Fig. 1.

Once effective masses, Dingle temperature and MB field are determined, frequency combinations can be considered. As evidenced in the few cases reported as examples in Fig. 3, data are nicely accounted for by the equations given in the appendix, with $g_\alpha=g_\beta=1.85\pm0.05$,

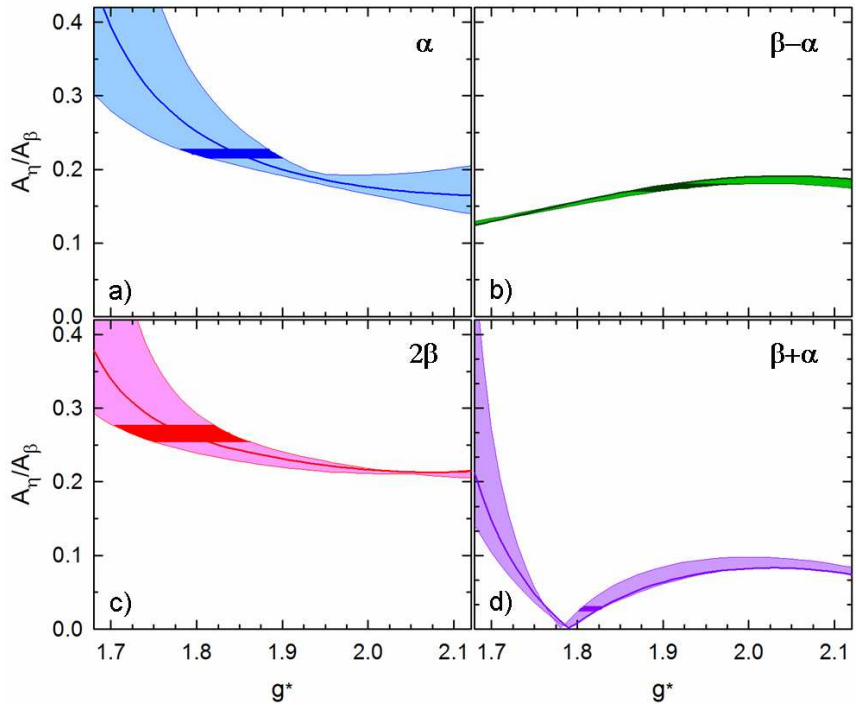

FIG. 4. (color on line) Influence of the effective Landé factor ($g^* = g_\alpha = g_\beta$, see text) on Fourier amplitudes A_η normalized to A_β for T=1.9 K and B=45 T. Solid lines are deduced from Eqs. (a) A.1, (b) A.5, (c) A.4 and (d) A.7 with the same parameters as in Figs. 2 and 3 (A_β is given by Eq. A.2). Lightly shaded areas accounts for the uncertainty on these parameters given in the text. Heavily shaded areas stand for experimental data, taking into account the experimental uncertainty: effective Landé factors in the range 1.7-2.0 account for these data.

which is just the value obtained for ET_4-Zn[9]. First, data for the 'forbidden frequency' $\beta-\alpha$, which only involve second order terms, is accounted for by the model. Next, strong deviation from the LK behaviour is noticed for the component $\beta+\alpha$ in Fig. 3(b). This behaviour, already observed for ET_4-Zn, is due to field- and temperature-dependent cancelation of the first and second order terms of Eq. A.7 in which the second order term dominated by the product $R_{\alpha,1}R_{\beta,1}$ come close to the first order term, dominated by $R_{\beta+\alpha,1}$. In the present case, a minimum amplitude can be inferred at a temperature below the explored range, whereas the minimum takes place around 2.5-3 K for ET_4-Zn in the field range 47-50 T[9].

To go further, it can be noticed in Fig. 1 that the amplitude of 2α is very small, hampering any data analysis in this case. In contrast, the amplitude of 2β is even larger than that linked to the basic orbit α. Contribution of the second order terms of Eqs. A.3 and A.4 is directly

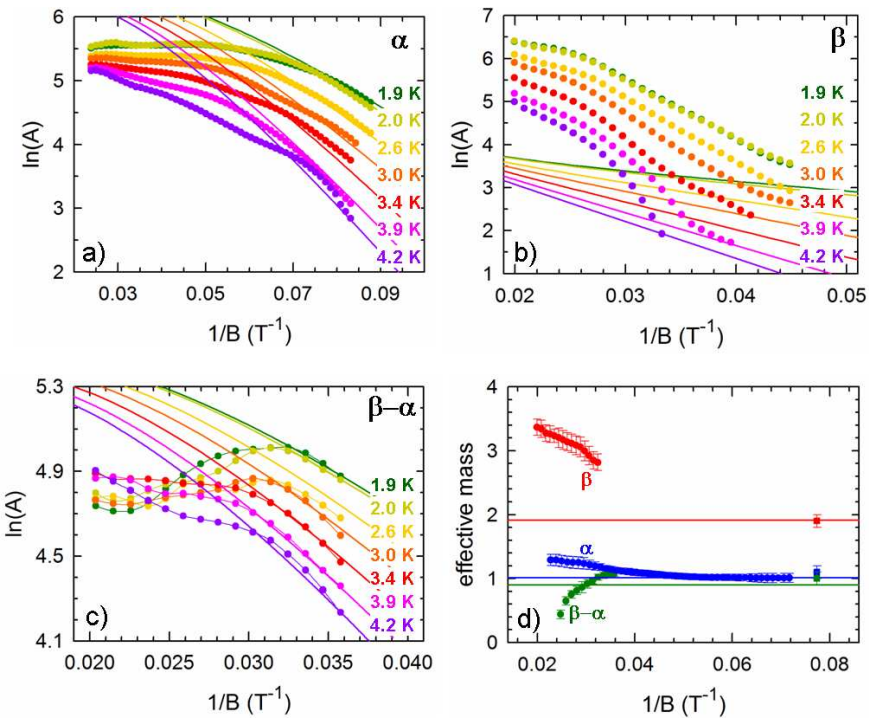

FIG. 5. (color on line) Dingle plots of (a) α, (b) β and (c) $\beta - \alpha$ components relevant to TDO data. Solid lines are best fits of the Lifshitz-Kosevich model to the data obtained with $m_\alpha(\theta = 0)$ = 1.00, $m_\beta(\theta = 0) = 1.88$ (which are the same as those deduced from dHvA data, see Fig. 2), $m_{\beta-\alpha}(\theta = 0) = 1.03$ and $T_D = 2$ K. Thin lines in (c) are guides to the eye. (d) Field dependence of the effective masses deduced from mass plots (not shown). Solid circles are deduced from the data in (a)-(c), solid squares are the values reported in Ref. 10. Horizontal lines correspond to the effective mass values m_α, m_β and $m_\beta - m_\alpha$ deduced from dHvA data of Fig. 2. Solid lines are obtained with the same effective masses and Dingle temperature as in panels (a)-(c).

responsible for these features. Regarding 2α, its behaviour is due to the almost cancelation of the first and second order terms which are dominated by $R_{\alpha,2}$ and $R^2_{\alpha,1}$, respectively (see Eq. A.3). Putting aside the spin damping factors ($R^s_{\alpha,2}$ and $R^s_{\alpha,1}$), these two factors are close to each other (they are actually equal as T/B goes to infinity). Owing to the tilt angle θ=10°, $R^s_{\alpha,2} = 0.90\pm0.03$ is very close to ${R^s_{\alpha,1}}^2 = 0.95\pm0.03$. Hence, taking into account the spin damping factors, the first and second order terms, which enter Eq. A.3 with an opposite sign, keep close values and have the same sign which accounts for the observed very small amplitude. This feature is at variance with many two-dimensional organic metals, in particular with ET_4-Zn and κ-$(ET)_2Cu(SCN)_2$ for which $R^s_{\alpha,2}$ is negative due to larger

effective mass. In contrast, a sizeable contribution of the second order terms of Eq. A.4 relevant to 2β is observed in Fig. 3(a). This is mainly due to a much smaller value of the spin damping factor $R^s_{\beta,2}$ compared to ${R^s_{\beta,1}}^2$ ($R^s_{\beta,2}/{R^s_{\beta,1}}^2 = 0.2$ for $g_\beta = 1.85$) entering Eq. A.4.

These findings lead us to discuss the absolute values of the Fourier amplitudes, in which spin damping factors, hence effective Landé factors play a key role. Since all the Fourier components are known within a constant factor (τ_0), ratios A_η/A_β are considered instead in the following. Fig. 4, in which shaded areas account for the uncertainties on the effective masses, MB field and Dingle temperature, display the Landé factor dependence (where it is assumed that $g_\alpha = g_\beta$, see above) of such ratios calculated from Eqs. A.1 to A.8. As it can be observed, values in agreement with experimental data are obtained for $g_\alpha = g_\beta = 1.85 \pm 0.15$, in nice agreement with the value deduced from the field and temperature dependence of the amplitudes (see fig. 3) albeit with a larger uncertainty.

Turn on now on SdH oscillations which are observed in TDO data. The main feature of these data is the number of frequency combinations observed in Fig. 1, even larger than for magnetic torque data. Dingle plots for α are displayed in Fig. 5(a). Solid lines in this figure are best fits of the LK formula to the data in the low field range (keeping in mind that, as reported above, the LK model holds for the α and β components amplitude of dHvA spectra). They are obtained with the effective masses and MB field derived from the dHvA oscillations and $T_D = 2$K (remember that T_D is the only sample-dependent parameter). Even though the field dependence is accounted for by the model in the low field range, strong deviations are noticed as the magnetic field increases. This behaviour, which is even more pronounced for β (see Fig. 5(b)) results in apparent field-dependent effective masses displayed in Fig. 5(d), which tend towards the values derived from both the above dHvA and the low field magnetoresistance data of Ref. 10 as the magnetic field decreases. Noticeably, the low field part of the TDO data relevant to $\beta - \alpha$ is accounted for by $m_{\beta-\alpha} = 1.0 \pm 0.2$ which is close to $m_\beta - m_\alpha = 0.88 \pm 0.13$, hence compatible with QI. This feature confirms once again[8,9] that the TDO technique is actually sensitive to conductivity rather than magnetization. This being said, not to mention QI oscillations, the analytical model which account for dHvA amplitudes is clearly not suitable for SdH oscillations at high field which still require a specific model.

IV. SUMMARY AND CONCLUSION

As expected for compounds with FS illustrating the linear chain of coupled orbits, dHvA and SdH spectra of θ-$(BETS)_4CoBr_4(C_6H_4Cl_2)$ are composed of many linear combinations of the frequencies linked to the α and β orbits. Compared to previously studied θ-phase organic metals ET_4-Co[8] and ET_4-Zn[9], smaller effective masses ($m_\alpha = 1.00\pm0.05$, $m_\beta = 1.88\pm0.08$) and MB field ($B_0 = 11.6\pm3.2$ T) are observed, allowing the observation of many frequency combinations in dHvA and SdH spectra in high magnetic fields.

As already reported for other compounds with the same FS topology, analytical formulas reported in the appendix, which are based on a second order development of the free energy within the canonical ensemble, account for the field and temperature dependence of the dHvA amplitudes with Landé factors equal, within error bars, to that derived from dHvA data of ET_4-Zn ($g_\alpha = g_\beta$=1.85±0.05). In particular, besides the 'forbidden frequency' $\beta - \alpha$ amplitude, the non-monotonic behaviour of $\beta + \alpha$ is nicely reproduced.

Beyond the field and temperature dependence of the amplitude, the strong influence of the spin damping factor, hence of the Landé factors, on the absolute value of the amplitudes is emphasized. In that respect, specific behaviours due to small effective masses such as the large amplitude of 2β and the small amplitude of 2α compared to that linked to the basic orbit β are quantitatively interpreted.

In contrast, the analytical model suitable for dHvA amplitudes cannot account for magnetoresistance oscillations measured by TDO technique at high field. A specific model is therefore still required for SdH oscillations of the linear chain of coupled orbits.

ACKNOWLEDGMENTS

Work in Toulouse was supported by the European Magnetic Field Laboratory (EMFL). Support of the project of Presidium RAS 0089-2015-0144 is acknowledged.

Appendix: Analytical expressions of Fourier amplitudes

Analytical expressions of dHvA amplitudes relevant to the linear chain of coupled orbits[7–9] are recalled in this appendix. Fourier amplitude $A_{p\eta}$ of the component with frequency $F_{p\eta} = p(n_\beta F_\beta \pm n_\alpha F_\alpha)$, where $n_{\alpha(\beta)}$ is the number of $\alpha(\beta)$ orbits involved in the or-

bit η and p is the harmonic number, depends on expressions involving damping factors $R_{\eta,p}(B,T) = R^T_{\eta,p}(B,T)R^D_{\eta,p}(B)R^{MB}_{\eta,p}(B)R^s_{\eta,p}$, given by the LK and coupled orbits network models[5,6]. The temperature damping factor is expressed as $R^T_{\eta,p} = pu_\eta \sinh^{-1}(pX_\eta)$, where $u_\eta = u_0 m_\eta T/B\cos\theta$, $u_0 = 2\pi^2 k_B m_e (e\hbar)^{-1} = 14.694$ T/K, θ is the angle between the magnetic field direction and the normal to the conducting plane and $m_\eta = n_\alpha m_\alpha + n_\beta m_\beta$ is the effective mass. The Dingle factor is given by $R^D_{\eta,p} = \exp(-pu_0 m_\eta T_D/B\cos\theta)$, where $T_D = \hbar(2\pi k_B\tau)^{-1}$ is the Dingle temperature and τ^{-1} is the scattering rate. MB contribution is accounted for by $R^{MB}_{\eta,p} = (ip_0)^{n^t_\eta}(q_0)^{n^r_\eta}$ where B_0 is the MB field in which the tunneling (p_0) and reflection (q_0) probabilities are given by $p_0 = \exp(-B_0/2B\cos\theta)$ and $p_0^2 + q_0^2 = 1$. Finally, the spin damping factor is given by $R^s_{\eta,p} = \cos(\pi g_\eta m_\eta/2\cos\theta)$, where g_η is the effective Landé factor.

$$A_\alpha = \frac{F_\alpha}{\pi m_\alpha}R_{\alpha,1} + \frac{F_\alpha}{2\pi m_\beta}R_{\alpha,1}R_{\alpha,2} + \cdots \tag{A.1}$$

$$A_\beta = \frac{F_\beta}{\pi m_\beta}R_{\beta,1} + \frac{F_\beta}{\pi m_\beta}R_{\alpha,1}R_{\beta+\alpha,1} + \cdots \tag{A.2}$$

$$A_{2\alpha} = -\frac{F_\alpha}{2\pi m_\alpha}R_{\alpha,2} + \frac{F_\alpha}{\pi m_\beta}\left[R^2_{\alpha,1} - \frac{2}{3}R_{\alpha,1}R_{\alpha,3}\right] + \cdots \tag{A.3}$$

$$A_{2\beta} = -\frac{F_\beta}{2\pi m_\beta}\left[R_{\beta,2} + 2R_{2\beta,1}\right] + \frac{F_\beta}{\pi m_\beta}\left[R^2_{\beta,1} + 2R_{\alpha,1}R_{2\beta-\alpha,1}\right] + \cdots \tag{A.4}$$

$$A_{\beta-\alpha} = -\frac{F_\beta - F_\alpha}{\pi m_\beta}\left[R_{\alpha,1}R_{\beta,1} + \frac{1}{2}R_{\alpha,2}R_{\alpha+\beta,1}\right] + \cdots \tag{A.5}$$

$$A_{2(\beta-\alpha)} = -\frac{2(F_\beta - F_\alpha)}{\pi m_\beta}\left[2R_{\alpha,1}R_{2\beta-\alpha,1} + R_{\alpha,2}(R_{2\beta,1} + \frac{1}{2}R_{\beta,2})\right] + \cdots \tag{A.6}$$

$$A_{\beta+\alpha} = -\frac{F_\beta + F_\alpha}{\pi(m_\beta + m_\alpha)}R_{\beta+\alpha,1} + \frac{F_\beta + F_\alpha}{\pi m_\beta}R_{\alpha,1}(R_{\beta,1} - R_{\beta+2\alpha,1}) + \cdots \tag{A.7}$$

$$A_{2\beta-\alpha} = -\frac{2F_\beta - F_\alpha}{\pi(2m_\beta - m_\alpha)}R_{2\beta-\alpha,1} - \frac{2F_\beta - F_\alpha}{\pi m_\beta}R_{\alpha,1}(\frac{1}{2}R_{\beta,2} + R_{2\beta,1}) + \cdots \tag{A.8}$$

It can be noticed that the terms of first order in damping factors correspond to the LK model. The minus signs account for π dephasing at turning points[13]. With regards to Eq. A.4, while $R_{\beta,2}$ stands for the second harmonic of β, $R_{2\beta,1}$ is the damping factor of a MB orbit with frequency $F_{2\beta}$ as discussed in Ref. 13. The same spin damping factor holds for both of them.

Second order terms relevant to the Fourier component $F_{n_\beta\beta\pm n_\alpha\alpha}$ arise from an infinite series of damping factors product $R_{\eta_1,p_1}R_{\eta_2,p_2}$ where $|p_1\eta_1 \pm p_2\eta_2| = n_\beta\beta \pm n_\alpha\alpha$. In Eqs. A.1

to A.8, only the very first terms with largest damping factors, which are not insignificant are reported.

---

[1] A. B. Pippard, Quantization of Coupled Orbits in Metals, Proc. Roy. Soc. (London) **A270** 1 (1962).

[2] H. Urayama, H. Yamochi, G. Saito, K. Nozawa, T. Sugano, M. Kinoshita, S. Sato, K. Oshima, A. Kawamoto and J. Tanaka, A new ambient pressure organic superconductor based on BEDT-TTF with T_c higher than 10 K (T_c = 10.4 K), Chem. Lett. **1** 55 (1988).

[3] K. Oshima, T. Mori, H. Inokuchi, H. Urayama, H. Yamochi and G. Saito, Shubnikov-de Haas effect and the Fermi surface in an ambient-pressure organic superconductor [bis(ethylenedithiolo)tetrathiafulvalene]$_2$Cu(NCS)$_2$, Phys. Rev. B **38** 938 (1988).

[4] S. Uji and J. S. Brooks, Physical Properties of Quasi-Two-Dimensional Organic Conductors in Strong Magnetic Fields, The Physics of Organic Superconductors and Conductors, Springer Series Material Science Vol. 110 (Springer, 2008), p. 89.

[5] L. M. Falicov and H. Stachowiak, Theory of de Haas-van Alphen effect in a system of coupled orbits. Application to magnesium, Phys. Rev. **147** 505 (1966).

[6] D. Shoenberg, Magnetic Oscillations in Metals (Cambridge University Press, Cambridge, 1984).

[7] A. Audouard, J.-Y. Fortin, D. Vignolles, V. N. Laukhin, N. D. Kushch and E. B. Yagubskii, New insights on frequency combinations and forbidden frequencies in the de Haas-van Alphen spectrum of κ-(ET)$_2$Cu(SCN)$_2$, J. Phys.: Condens. Matter **28** 275702 (2016).

[8] A. Audouard, J.-Y. Fortin, D. Vignolles, R. B. Lyubovskii, L. Drigo, F. Duc, G. V. Shilov, G. Ballon, E. I. Zhilyaeva, R. N. Lyubovskaya and E. Canadell, Quantum oscillations in the linear chain of coupled orbits: The organic metal with two cation layers θ-(ET)$_4$CoBr$_4$(C$_6$H$_4$Cl$_2$), EPL **97** 57003 (2012).

[9] A. Audouard, J.-Y. Fortin, D. Vignolles, R. B. Lyubovskii, L. Drigo, G. V. Shilov, F. Duc, E. I. Zhilyaeva, R. N. Lyubovskaya and E. Canadell, Non-Lifshitz-Kosevich field- and temperature-dependent amplitude of quantum oscillations in the quasi-two dimensional metal θ-(ET)$_4$ZnBr$_4$(C$_6$H$_4$Cl$_2$), J. Phys.: Condens. Matter **27** 315601 (2015).

[10] R. B. Lyubovskii, S. I. Pesotskii, G. V. Shilov, E. I. Zhilyaeva, A. M. Flakina and R. N. Lyubovskaya, Shubnikov-de Haas Oscillations in a New Dual Layered Quasi Two Dimensional

Organic Metal $(BETS)_4CoBr_4(C_6H_4Cl_2)$, JETP Letters **98** 181 (2013).

[11] G.V. Shilov, E.I. Zhilyaeva, A.M. Flakina, S.A. Torunova, R.B. Lyubovskii, S.M. Aldoshin and R.N. Lyubovskaya, Phase transition at 320 K in new layered organic metal $(BEDT\text{-}TTF)_4CoBr_4(C_6H_4Cl_2)$, Cryst. Eng. Comm. **13** 1467 (2011).

[12] L. Drigo, F. Durantel, A. Audouard and G. Ballon, Tunnel diode oscillator-based measurement of quantum oscillations amplitude in pulsed high magnetic fields: a quantitative field-dependent study, Eur. Phys. J.-Appl. Phys. **52** 10401 (2010).

[13] A. Audouard and J.-Y. Fortin, Recent developments in the determination of the amplitude and phase of quantum oscillations for the linear chain of coupled orbits, Low Temp. Phys. (2014), [Fiz. Nizk. Temp. **40** (2014)].